Euro. Jnl of Applied Mathematics (2019), *vol.* 30, *pp.* 1025–1037 © Cambridge University Press 2018.
doi:10.1017/S0956792518000670

Chaotic backward shift operator on Chebyshev polynomials

MÁRTON KISS[1] and TAMÁS KALMÁR-NAGY[2]

[1]*Department of Differential Equations, Institute of Mathematics, Budapest University of Technology and Economics, H 1111 Budapest, Műegyetem rkp. 3-9, Hungary*
email: mkiss@math.bme.hu
[2]*Department of Fluid Mechanics, Faculty of Mechanical Engineering, Budapest University of Technology and Economics, H 1111 Budapest, Műegyetem rkp. 3-9, Hungary*
email: ejam@kalmarnagy.com

(*Received 12 February 2018*; *revised 16 September 2018*; *accepted 22 November 2018*; *first published online 21 December 2018*)

We obtain the representation of the backward shift operator on Chebyshev polynomials involving a principal value (PV) integral. Twice the backward shift on the space of square-summable sequences l^2 displays chaotic dynamics, thus we provide an explicit form of a chaotic operator on $L_2\left(-1, 1, \left(1-x^2\right)^{-1/2}\right)$ using Cauchy's PV integral. We explicitly calculate the periodic points of the operator and provide examples of unbounded trajectories, as well as chaotic ones. Histograms and recurrence plots of shifts of random Chebyshev expansions display interesting behaviour over fractal measures.

Key words: Backward shift, principal value integral, Chebyshev polynomials

2010 Mathematics Subject Classification: 34A55, 34B20, 34B24, 34B45 (Primary); 34L40, 47A75 (Secondary)

1 Introduction

While finite dimensional linear systems have been well understood, infinite dimensional linear systems can have surprisingly complex dynamics. Almost 50 years ago, Rolewicz [31] demonstrated that a linear operator (the backward shift multiplied by 2) on the space of square-summable sequences l_2 exhibits transitivity.

Thus nonlinearity is NOT a requirement for chaotic dynamics. Nice exposition of dynamics of infinite-dimensional operators is given in Refs. [34], [12] and the books [1], [18].

Recent papers such as [22], [28] also explore the topic of complex behaviour of linear systems. Bernardes et al. [2] obtain new characterisations of Li–Yorke chaos for linear operators on Banach and Fréchet spaces.

While the backward shift example seems artificial, transitive operators are not rare. To wit, Herrero [21] and Chan [6] proved that chaotic linear operators are dense in the set of bounded linear operators. There are many examples of chaotic linear operators including weighted shifts [33], composition operators [3], and differentiation and translations [13, 15, 29].

The interest in backward shift operators increased with the notion of chaotic semigroups [17, 27, 30]. An example of a chaotic shift operator is provided in the form of a linear partial

https://doi.org/10.1017/S0956792518000670 Published online by Cambridge University Press

differential equation with both diffusion and transport by Desch et al. [8]. Gulisashvili and MacCluer [19] demonstrated that the annihilation operator for a linear quantum harmonic oscillator (a weighted shift operator) is chaotic. Conejero et al. [7] study a partial differential equation arising in the dynamics of linear vibrations of elastic structures. Other applications of shift operators include a wide range of topics, including scattering theory [11], and a model of blood production [9].

Our interest in representing and describing dynamics on infinite sequences is motivated by the Carleman embedding technique which embeds a nonlinear autonomous differential equation into an infinite system of linear ordinary differential equations [25]. Our aim is to recognise the signature of the shift operator in infinite dimensional linear systems and thereby demonstrating the occurrence of chaos in the associated nonlinear differential equations. We envision application of the method for analysing a sequence of measurements.

Based on Rolewicz's example, the authors of this paper constructed a chaotic operator on the space of 2π-periodic odd functions and provided its representation involving a principal value integral [23], and explicitly calculated the eigenfunction and periodic points of this operator.

In order to enrich the space of sequences with analytical structures, an idea is to represent the sequence as a Fourier series with respect to a given orthogonal system. The space l_∞ of bounded sequences has poor convergence properties: the series will not converge pointwise. Hence we work on l_2 instead. This can be justified as follows: take a sequence from l_∞ and a number $\alpha > 1$. Divide the n-th number of the sequence by α^n. Then we have a sequence in l_2.

In this paper we consider an infinite dimensional dynamical system on the Hilbert space of square-integrable functions with weight $w(x) = \frac{1}{\sqrt{1-x^2}}$, i.e. $L_2(-1, 1, w(x))$. This weight corresponds to Chebyshev functions. If $f(x)$ is Lipschitz continuous on $[-1, 1]$, it has a uniformly and absolutely convergent Chebyshev series (Chebyshev expansion of functions has been discussed in [4]):

$$f(x) = \sum_{k=0}^{\infty} a_k T_k(x), \quad a_0 = \frac{1}{\pi}\int_{-1}^{1} f(x)\frac{dx}{\sqrt{1-x^2}},$$

$$a_k = \frac{2}{\pi}\int_{-1}^{1} f(x)\, T_k(x)\frac{dx}{\sqrt{1-x^2}} \quad (k \geq 1). \tag{1.1}$$

Here we construct a chaotic linear operator by 'lifting' $2B$ to the space $L_2\left(-1, 1, \frac{1}{\sqrt{1-x^2}}\right)$.

In Section 2 we explicitly construct the backward shift on $L_2\left(-1, 1, \frac{1}{\sqrt{1-x^2}}\right)$ in terms of a PV integral. In Section 3 we define and analyse the corresponding chaotic operator $\mathcal{C}$, including finding its eigenvectors and periodic points. We provide examples of unbounded and chaotic trajectories of $\mathcal{C}$. Section 4 concludes the paper.

2 Backward shift on Chebyshev polynomials

Chebyshev polynomials are defined by $T_n(\cos t) = \cos(nt)$ $(n \geq 0)$. They are widely used in many areas of numerical analysis: interpolation theory, uniform approximation, least-squares approximation, numerical solution of ordinary and partial differential equations (the so-called spectral or pseudospectral methods) [16].

https://doi.org/10.1017/S0956792518000670 Published online by Cambridge University Press

With the change of variable $x = \cos t$ the Chebyshev polynomials $T_n(x)$ have the following properties:

- satisfy the recurrence relation $T_{n+1}(x) = 2xT_n(x) - T_{n-1}(x)$;
- have leading coefficient 2^{n-1} and $T_n(-x) = (-1)^n T_n(x)$;
- have n zeros in the interval $(-1, 1)$ given by $T_n(\cos\left(\frac{2k+1}{2n}\pi\right)) = 0$, $(k = 0, 1, \ldots, n-1)$;
- have $n+1$ extrema in the interval $[-1, 1]$ given by $T_n(\cos\left(\frac{k}{n}\pi\right)) = (-1)^k$, $(k = 0, 1, \ldots, n)$;
- form a complete orthogonal system in $L^2(-1, 1, w(x))$, $w(x) = (1-x^2)^{-\frac{1}{2}}$;
- satisfy the Rodriguez-type formula

$$T_n(x) = \frac{(-1)^n 2^n n!}{(2n)!}\sqrt{1-x^2}\frac{\mathrm{d}^n}{\mathrm{d}x^n}[(1-x^2)^{n-\frac{1}{2}}].$$

The backward shift B on Chebyshev polynomials is an $L^2(-1, 1, w(x)) \to L^2(-1, 1, w(x))$ continuous linear operator which maps $T_n(x)$ to $T_{n-1}(x)$ (with the convention $T_{-1}(x) = 0$). Substituting $x = \cos t$, the space $L^2(-1, 1, w(x))$ with the Chebyshev basis is isomorphic to $L^2(0, \pi)$ with the cosine basis. Let us define the backward shift operator $\mathcal{B}$ as a continuous linear operator on the space of even square-integrable 2π-periodic functions which satisfies $\mathcal{B}\cos nt = \cos(n-1)t$ for $n \geq 1$ and $\mathcal{B}1 = 0$.

Theorem 2.1 *The backward shift on Chebyshev polynomials can be represented by*

$$\mathcal{B}F(x) = F(x)x + \frac{1}{\pi}\mathrm{PV}\int_{-1}^{1}\frac{1-xy}{y-x}F(y)\frac{\mathrm{d}y}{\sqrt{1-y^2}}. \tag{2.1}$$

We recall that the PV integral (see i.e., [5], p. 457) of a function f about a point $c \in (a, b)$ is given by

$$\mathrm{PV}\int_a^b f(x)dx = \lim_{\varepsilon\to 0+}\left(\int_a^{c-\varepsilon} f(x)dx + \int_{c+\varepsilon}^b f(x)dx\right). \tag{2.2}$$

Let us substitute $y = \cos\xi$, $F(y) = f(\xi)$ into the second term of (2.1) (the change of variables is justified as in [14], p. 17). This gives an isometry from $L^2(-1, 1, w(x))$ to $L^2(0, \pi)$. With $x = \cos t$ we get (2.3) after rearranging. Hence the statement of Theorem 2.1 is equivalent to the following:

Theorem 2.2 *The backward shift operator on the space of even square-integrable 2π-periodic functions (i.e., on the space $L^2(0, \pi)$ with basis $\{1, \cos nt : n \geq 1\}$) can be represented by*

$$\mathcal{B}f(t) = f(t)\cos t + \frac{1}{\pi}\mathrm{PV}\int_0^{\pi}\frac{1-\cos\xi\cos t}{\cos\xi - \cos t}f(\xi)d\xi. \tag{2.3}$$

Lemma 2.3 *The backward shift operator on the space of even square-integrable 2π-periodic functions with basis $\{1, \cos nt : n \geq 1\}$ can be expressed as*

$$\mathcal{B}f(t) = \left(f(t) - \frac{1}{\pi}\int_0^{\pi} f(\xi)d\xi\right)\cos t + (\mathcal{H}f(t))\sin t \quad (n \geq 1), \tag{2.4}$$

where $\mathcal{H}$ is the Hilbert transform:

$$\mathcal{H}f(t) = \frac{1}{\pi}\mathrm{PV}\int_{-\infty}^{\infty}\frac{f(\tau)}{t-\tau}\mathrm{d}\tau. \tag{2.5}$$

https://doi.org/10.1017/S0956792518000670 Published online by Cambridge University Press

Proof The Hilbert transform maps the real part of a complex differentiable function on the upper half plane to its imaginary part. In particular, $\mathcal{H}\cos nt = \sin nt$ $(n \geq 0)$, hence

$$\mathcal{B}\cos nt = \cos nt \cos t + (\mathcal{H}\cos nt)\sin t \quad (n \geq 1), \tag{2.6}$$

$$\mathcal{B}1 = 0 = (\mathcal{H}1)\sin t \quad (n = 0). \tag{2.7}$$

Thus the two sides of (2.4) agree if $f(t)$ is a basis element. By linearity and continuity, they are equal for all $f(t) \in L^2(0, \pi)$. □

Proof of Theorem 2.2 Let us recall the formula for the Hilbert transform of periodic functions ([24], pp. 114, 528; [26], p. 18; [20], p. 21; [32], p. 262):

$$\mathcal{H}f(t) = \frac{1}{2\pi}\mathrm{PV}\int_{-\pi}^{\pi} \cot\left(\frac{t-\xi}{2}\right) f(\xi)d\xi = \frac{1}{2\pi}\mathrm{PV}\int_{-\pi}^{\pi} \frac{\sin t + \sin\xi}{\cos t - \cos\xi} f(\xi)d\xi. \tag{2.8}$$

If f is an even function, (2.8) can be transformed to

$$\mathcal{H}f(t) = \frac{1}{2\pi}\mathrm{PV}\int_{-\pi}^{\pi} \frac{\sin t}{\cos t - \cos\xi} f(\xi)d\xi = \frac{1}{\pi}\mathrm{PV}\int_{0}^{\pi} \frac{\sin t}{\cos t - \cos\xi} f(\xi)d\xi. \tag{2.9}$$

Using (2.4) leads to

$$\mathcal{B}f(t) = \left(f(t) - \frac{1}{\pi}\int_0^{\pi} f(\xi)d\xi\right)\cos t + \frac{1}{\pi}\mathrm{PV}\int_0^{\pi} \frac{\sin^2 t}{\cos\xi - \cos t} f(\xi)d\xi, \tag{2.10}$$

which is the same as (2.3). □

We now define our 'chaotic' operator (twice the backward shift) as

$$\mathcal{C}F(x) := 2\mathcal{B}F(x) = 2F(x)x + \frac{2}{\pi}\mathrm{PV}\int_{-1}^{1} \frac{1-xy}{y-x} F(y)\frac{\mathrm{d}y}{\sqrt{1-y^2}}. \tag{2.11}$$

In the following we discuss the chaotic operator $\mathcal{C}$.

3 Analysis of the Chaotic operator $\mathcal{C}$

Consider the Chebyshev expansion of a function

$$F(x) = \sum_{n=0}^{\infty} a_n T_n(x). \tag{3.1}$$

The eigenfunctions of $\mathcal{C}$ can be found from the eigenvalue relation

$$\mathcal{C}F^*(x) = \lambda F^*(x). \tag{3.2}$$

Instead of using equation (2.11), we revert to equation (1.1) to write

$$\sum_{n=0}^{\infty} 2a_{n+1}T_n(x) = \sum_{n=0}^{\infty} \lambda a_n T_n(x). \tag{3.3}$$

From this we have

$$a_{n+1} = \left(\frac{\lambda}{2}\right) a_n, \tag{3.4}$$

https://doi.org/10.1017/S0956792518000670 Published online by Cambridge University Press

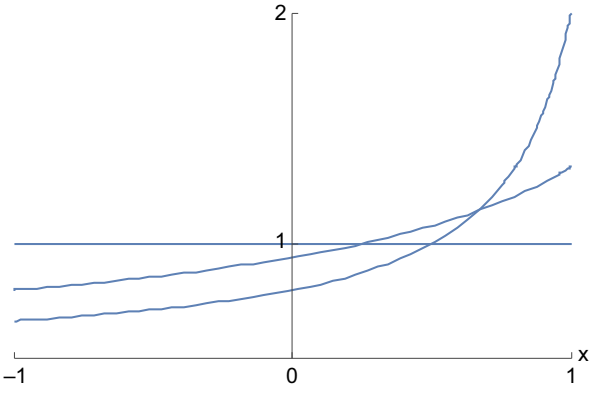


FIGURE 1. Eigenfunctions $\frac{4-2x\lambda}{\lambda^2-4x\lambda+4}$ for $\lambda = 0, 1/2, 1$.

and thus

$$F^*(x) = a_0 \sum_{n=0}^{\infty} \left(\frac{\lambda}{2}\right)^n T_n(x) = a_0 \frac{4-2x\lambda}{\lambda^2-4x\lambda+4}. \tag{3.5}$$

The functions corresponding to eigenvalue $\lambda = 1$ are

$$F^*(x) = a_0 \frac{4-2x}{5-4x}, \tag{3.6}$$

i.e., the functions $a_0 \frac{4-2x}{5-4x}$ are invariant under the action of $\mathcal{C}$. In other words $F^*(x)$'s are fixed points of operator $\mathcal{C}$. A family of eigenfunctions is displayed in Figure 1 (we set $a_0 = 1$). At the endpoints $F^*(\pm 1) = \frac{2}{2\mp\lambda}$.

To better characterise the action of $\mathcal{C}$ we want to understand how a given function is 'shaped' under the repeated application of $\mathcal{C}$. For $F \in L_2(-1, 1, w(x))$ the orbit of F is defined as $\text{Orb}(\mathcal{C}, F) = \{F, \mathcal{C}F, \mathcal{C}^2F, \ldots\}$ where $\mathcal{C}^k = \underbrace{\mathcal{C} \circ \ldots \circ \mathcal{C}}_{k}$ is the kth composition of $\mathcal{C}$ with itself. The k-fold composition acts on $F(x)$ as

$$\mathcal{C}^k F(x) = 2^k \sum_{n=0}^{\infty} a_{n+k} T_n(x). \tag{3.7}$$

A given $F \in L_2(-1, 1, w(x))$ is a Q-periodic point of $\mathcal{C}$ if $\mathcal{C}^Q f = f$ for the least such integer $Q \geq 1$ (a fixed point is a 1-periodic point, i.e. $Q = 1$). We are now in the position to construct Q-periodic points of $\mathcal{C}$.

Introducing $y = \{y_0, \ldots, y_{Q-1}\}$, a Q-periodic point of $2B$ (acting on l_2) can be written as [12]

$$a = \left(y_0, \ldots, y_{Q-1}, \frac{y_0}{2^Q}, \ldots, \frac{y_{Q-1}}{2^Q}, \frac{y_0}{2^{2Q}}, \ldots, \frac{y_{Q-1}}{2^{2Q}}, \ldots\right), \tag{3.8}$$

whose nth component is given by

$$a_n = \frac{y_{n \bmod Q}}{2^{[\frac{n}{Q}]Q}}. \tag{3.9}$$

https://doi.org/10.1017/S0956792518000670 Published online by Cambridge University Press

Using the linearity of $\mathcal{C}$ we can easily find a period-2 point of $\mathcal{C}$, i.e. a function $g(x)$ such that $\mathcal{C}^2 g(x) = g(x)$:

$$g(x) = y_0 \sum_{n=0}^{\infty} \frac{T_{2n}(x)}{2^{2n}} + y_1 \sum_{n=0}^{\infty} \frac{T_{2n+1}(x)}{2^{2n}} = y_0 \frac{12x}{25 - 16x^2} + y_1 \frac{8x^2 - 20}{25 - 16x^2}. \tag{3.10}$$

In general, we find a period-Q point of $\mathcal{C}$ as

$$f(t) = y_0 \left(T_0(x) + \frac{T_Q(x)}{2^Q} + \cdots + \frac{T_{nQ}(x)}{2^{nQ}} + \cdots \right) \tag{3.11}$$

$$+ y_1 \left(T_1(x) + \frac{T_{Q+1}(x)}{2^Q} + \cdots + \frac{T_{nQ+1}(x)}{2^{nQ}} + \cdots \right) + \cdots + \tag{3.12}$$

$$+ y_{Q-1} \left(T_{Q-1}(x) + \frac{T_{2Q-1}(x)}{2^Q} + \cdots + \frac{T_{(n+1)Q-1}(x)}{2^{nQ}} + \cdots \right) \tag{3.13}$$

By defining the 'basis-functions,'

$$\phi\,(l, Q) = \sum_{n=0}^{\infty} \frac{T_{nQ+l}(x)}{2^{nQ}} = \mathrm{Re}\, \frac{(x + i\sqrt{1 - x^2})^l}{1 - 2^{-Q}(x + i\sqrt{1 - x^2})^Q}, \tag{3.14}$$

a period-Q point of $\mathcal{C}$ can be expressed as the linear combination

$$f(x) = \sum_{l=0}^{Q-1} y_l \phi(l, Q). \tag{3.15}$$

The first few basis functions are (shown in Figure 2)

$$Q = 1, \qquad \phi(0, 1) = \frac{2x - 4}{4x - 5} \tag{3.16}$$

$$Q = 2, \qquad \phi(0, 2) = \frac{8x^2 - 20}{16x^2 - 25}, \qquad \phi(1, 2) = \frac{-12x}{16x^2 - 25}, \tag{3.17}$$

$$Q = 3, \qquad \phi(0, 3) = \frac{32x^3 - 24x - 64}{64x^3 - 48x - 65}, \qquad \phi(1, 3) = \frac{16x^2 - 64x - 8}{64x^3 - 48x - 65}, \tag{3.18}$$

$$\phi(2, 3) = \frac{-128x^2 + 8x + 64}{64x^3 - 48x - 65}$$

$$Q = 4, \qquad \phi(0, 4) = \frac{128x^4 - 128x^2 - 240}{256x^4 - 256x^2 - 225}, \qquad \phi(1, 4) = \frac{64x^3 - 304x}{256x^4 - 256x^2 - 225}, \tag{3.19}$$

$$\phi(2, 4) = \frac{-480x^2 + 240}{256x^4 - 256x^2 - 225}, \qquad \phi(3, 4) = \frac{-1024x^3 + 784x}{256x^4 - 256x^2 - 225}.$$

Now we examine the effect of $\mathcal{C}$ on some functions, namely the square wave, the semi-circle and Whittaker's cardinal function (Sinc). The Chebyshev series of these functions are the following:

https://doi.org/10.1017/S0956792518000670 Published online by Cambridge University Press

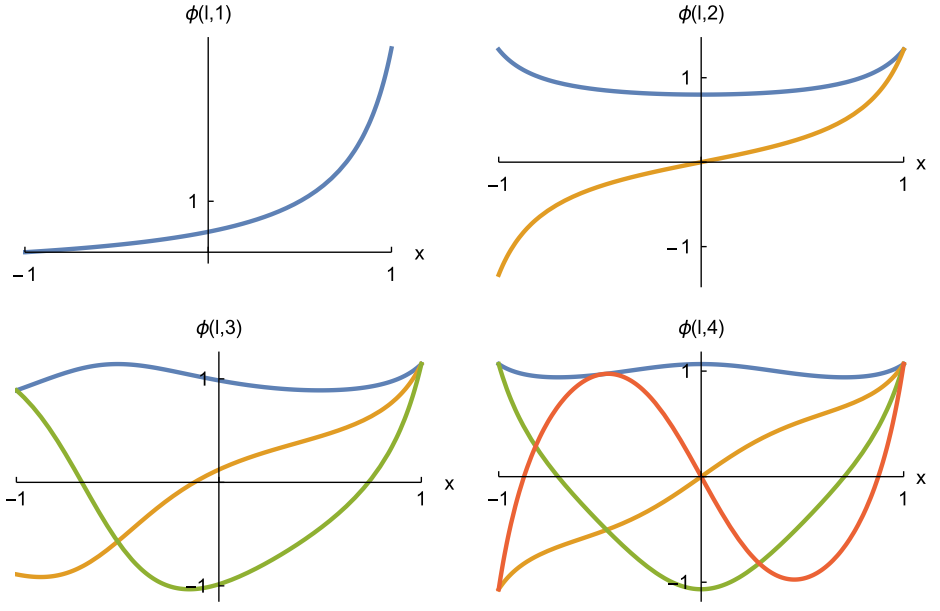


FIGURE 2. Basis functions $\phi(l, T)$ for $T = 1, \ldots, 4,\ l = 0, \ldots, T-1$.

$$\mathrm{Sqw}(x) = \begin{cases} -\frac{1}{2} & -1 < x < 0 \\ \frac{1}{2} & 0 < x < 1 \end{cases} = \sum_{k=1}^{\infty} \frac{2}{k\pi} \sin\left(\frac{k\pi}{2}\right) T_k(x), \tag{3.20}$$

$$\mathrm{Circle}(x) = \sqrt{1-x^2} = \frac{2}{\pi}\left(1 + \sum_{k=2}^{\infty} \frac{1+\cos(k\pi)}{1-k^2} T_k(x)\right), \tag{3.21}$$

$$\mathrm{Sinc}(x) = \frac{\sin 4\pi x}{4\pi x} = a_0 T_0(x) + a_2 T_2(x) + a_4 T_4(x) + \cdots, \tag{3.22}$$

where the coefficients can be expressed in terms of Bessel functions J_n and Struve functions H_n. For example

$$a_0 = \frac{1}{2}\pi^2 H_0(4\pi) J_1(4\pi) + \left(\pi - \frac{1}{2}\pi^2 H_1(4\pi)\right) J_0(4\pi). \tag{3.23}$$

Figure 3 shows the first seven elements of the orbits of these functions. Even though initially the norms of the iterates grow, in general this only holds for our first two examples. For $\mathrm{Sqw}(x)$, $\lim_{k\to\infty} |\frac{a_{2k+1}}{a_{2k-1}}| = 1$, hence for each $1 < \alpha < 2$, $\frac{\alpha^{2k+1}}{2^{2k+1}} |a_{2k+1}| \to 0$. Consequently

$$\|\mathcal{C}^n \mathrm{Circle}(x)\| \geq \frac{1}{\sqrt{\pi}} \max\{2^n |a_n|, 2^n |a_{n+1}|\} > \alpha^n \tag{3.24}$$

for n large enough. The second example ($\mathrm{Circle}(x)$) is similar as $\lim_{k\to\infty} |\frac{a_{2k+2}}{a_{2k}}| = 1$. In contrast to these functions, $\mathrm{Sinc}(x)$ has an orbit converging to zero under the action of $\mathcal{C}$. Integrating by parts in the Rodriguez formula (the last property of $T_n(x)$) one gets [10]

$$|a_n| \leq \frac{1}{2^{n-1} n!} \max_{-1 \leq x \leq 1} |f^{(n)}(x)|. \tag{3.25}$$

https://doi.org/10.1017/S0956792518000670 Published online by Cambridge University Press

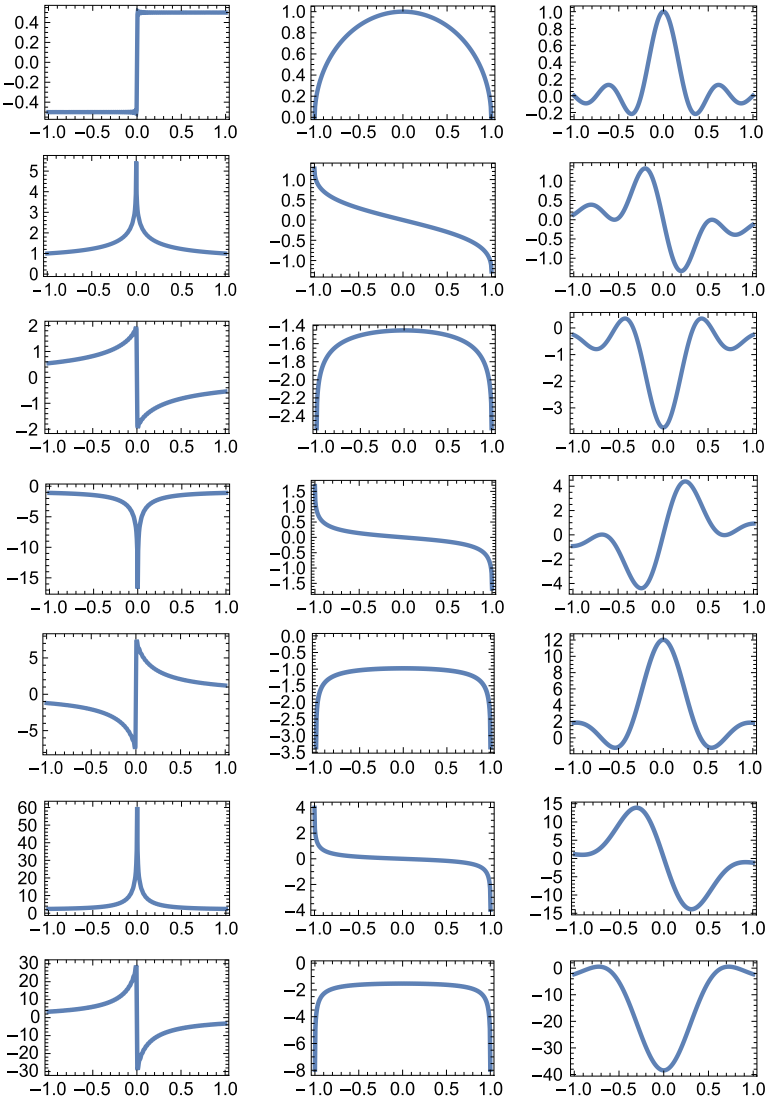


FIGURE 3. Iterates of the square-wave, semicircle and sinc functions.

Power series expansion of $f(x) = \frac{\sin 4\pi x}{4\pi x}$ shows that

$$|f^{(n)}(x)| = \left| \sum_{k \geq n/2} \frac{1}{2k+1} \frac{(4\pi)^{2k} x^{2k-n}}{(2k-n)!} \right| \leq \frac{e^{4\pi}}{n+1} (4\pi)^n \tag{3.26}$$

for $-1 \leq x \leq 1$. Hence for $N \geq 8$

$$\|\mathcal{C}^N f\|^2 \leq 4^N \pi \sum_{n=N}^{\infty} |a_n|^2 \leq 4^{N+1} \pi \sum_{n=N}^{\infty} \frac{(2\pi)^{2n}}{((n+1)!)^2} \leq 4^{N+2} \pi \frac{(2\pi)^{2N}}{((N+1)!)^2} \tag{3.27}$$

which tends to zero.

https://doi.org/10.1017/S0956792518000670 Published online by Cambridge University Press

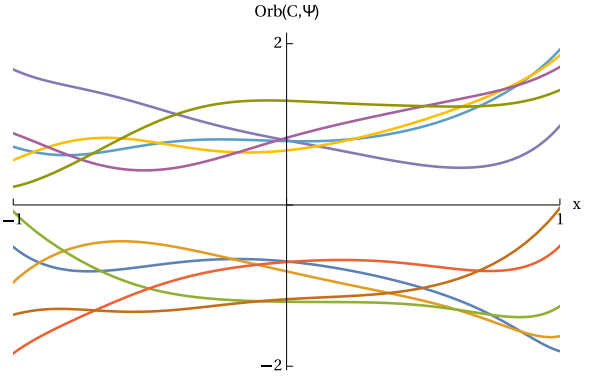


FIGURE 4. The first 10 elements of Orb $(\mathcal{C}, \Psi)$.

Now we turn to creating a function that gives rise to a chaotic orbit under the action of $\mathcal{C}$. First, we note that for $2B$ (on l_2) the point

$$y = \left(\frac{y_0}{1}, \frac{y_1}{2}, \frac{y_2}{4} \cdots\right), \tag{3.28}$$

where y_i is a random variable, generates a chaotic orbit. We now lift this point to L_2 $(-1, 1, w(x))$ using equation (3.1):

$$\Psi(x) = \sum_{i=0}^{\infty} \frac{y_i}{2^i} T_i(x). \tag{3.29}$$

Figure 4 shows the first 10 elements of the orbit of Ψ under the action of $\mathcal{C}$, i.e. Orb $(\mathcal{C}, \Psi)$, when the y's are randomly chosen (with 0.5 probability) from the set $\{-1, 1\}$. The first element of the orbit is Ψ itself.

Figure 5 shows the orbit Orb $(\mathcal{C}, \Psi)$ evaluated at three different x's $(1/20, 1/2, 19/20)$ for 100 iteration.

The histograms and recurrence plots ($\mathcal{C}^i\Psi(x)$ vs. $\mathcal{C}^{i-1}\Psi(x)$) are shown in Figure 6 for $x = 0, \frac{1}{4}, \frac{1}{2}, \frac{3}{4}, 1$.

The invariant measures and recurrences display fractal properties.

The bottom-left picture (corresponding to $x = 1$) in Figure 6 shows a uniform distribution. Indeed, as $T_n(1) = 1$ for all n, the probability density function is symmetric with respect to every dyadic number. The bottom-right picture shows that

- $\mathcal{C}^i\Psi(1) = 2(\mathcal{C}^{i-1}\Psi(1) \pm 1)$ depending on the ith digit of Ψ; and
- the numbers $\mathcal{C}^n\Psi(1)$ are uniformly distributed on $[-1, 1]$.

$T_n(0)$ is a 4-periodic sequence. It is zero for n odd, and ± 1 for n even. As the signs of digits of y_i are $+$ or $-$ with equal probability, we have random sums $\sum_{n=0}^{\infty} \frac{\pm 1}{4^n}$. Their distribution is symmetric to 0, ± 1, $\pm(1 \pm \frac{1}{4}), \ldots, \sum_{n=0}^{N} \frac{\pm 1}{4^n}$ and so on. The support of the invariant measure is a Cantor set, which is defined recursively as follows. $\sum_{n=0}^{\infty} \frac{1}{4^n} = \frac{4}{3}$, hence the support is contained in the interval $[-\frac{4}{3}, \frac{4}{3}]$. Let us take this interval and leave out its open middle third; and repeat this procedure for every line segment ad infinitum. The remaining set

https://doi.org/10.1017/S0956792518000670 Published online by Cambridge University Press

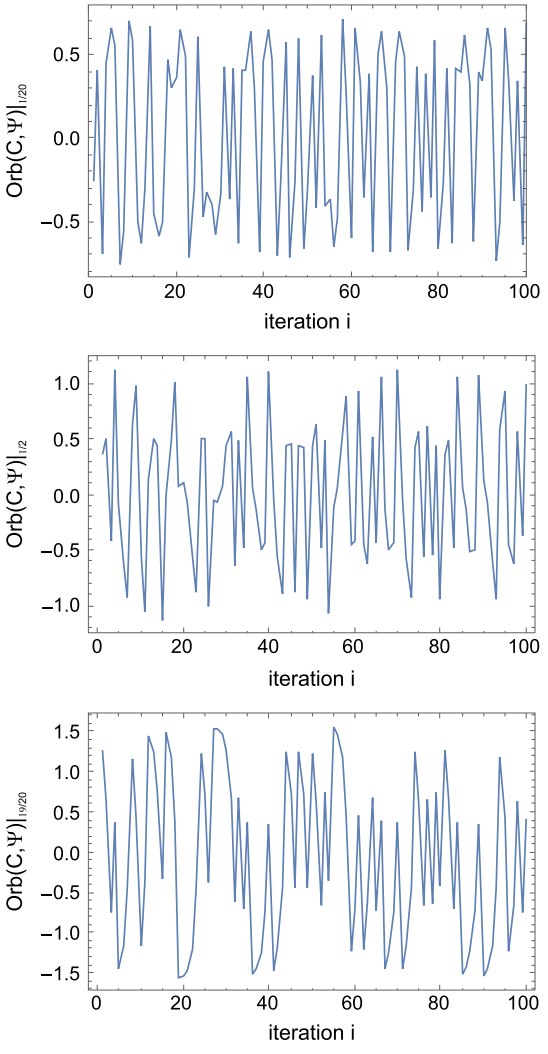


FIGURE 5. The first 100 elements of Orb $(\mathcal{C}, \Psi)$ at fixed x $(1/20, 1/2, 19/20)$.

contains exactly the sums $\sum_{n=0}^{\infty} \frac{\pm 1}{4^n}$. This is the top-left picture in Figure 6. The top-right picture shows that

- $\mathcal{C}^i\Psi(1) = 2(\mathcal{C}^{i-1}\Psi(1) \pm 1)$ or $2\mathcal{C}^{i-1}\Psi(1)$ depending on the ith digit of Ψ; and
- the numbers $\mathcal{C}^n\Psi(1)$ are uniformly distributed on the Cantor set described above.

$T_n(\frac{1}{2})$ is a 6-periodic sequence $\{1, \frac{1}{2}, -\frac{1}{2}, -1, -\frac{1}{2}, \frac{1}{2}\}$ from $n = 0$. The suport of the invariant measure is a more complicated Cantor set (middle-left picture in Figure 6). The middle-right picture also shows the support and that $\mathcal{C}^i\Psi(1) = 2(\mathcal{C}^{i-1}\Psi(1) \pm 1)$ or $\mathcal{C}^i\Psi(1) = 2(\mathcal{C}^{i-1}\Psi(1) \pm \frac{1}{2})$ depending on the ith digit of Ψ in this case.

Finally, $T_n(\frac{1}{4})$ and $T_n(\frac{3}{4})$ are themselves uniformly distributed sequences on $[-1, 1]$. If we permitted sums like $\sum_{i=0}^{\infty} \frac{y_i}{2^i} T_{\sigma(i)}(x)$, where σ is a permutation, we would get a uniform distribution. But as the first term in the sum $\sum_{i=0}^{\infty} \frac{y_i}{2^i} T_i(x)$ is always ± 1 and the sum of remaining terms are strictly less, there are holes in the support.

https://doi.org/10.1017/S0956792518000670 Published online by Cambridge University Press

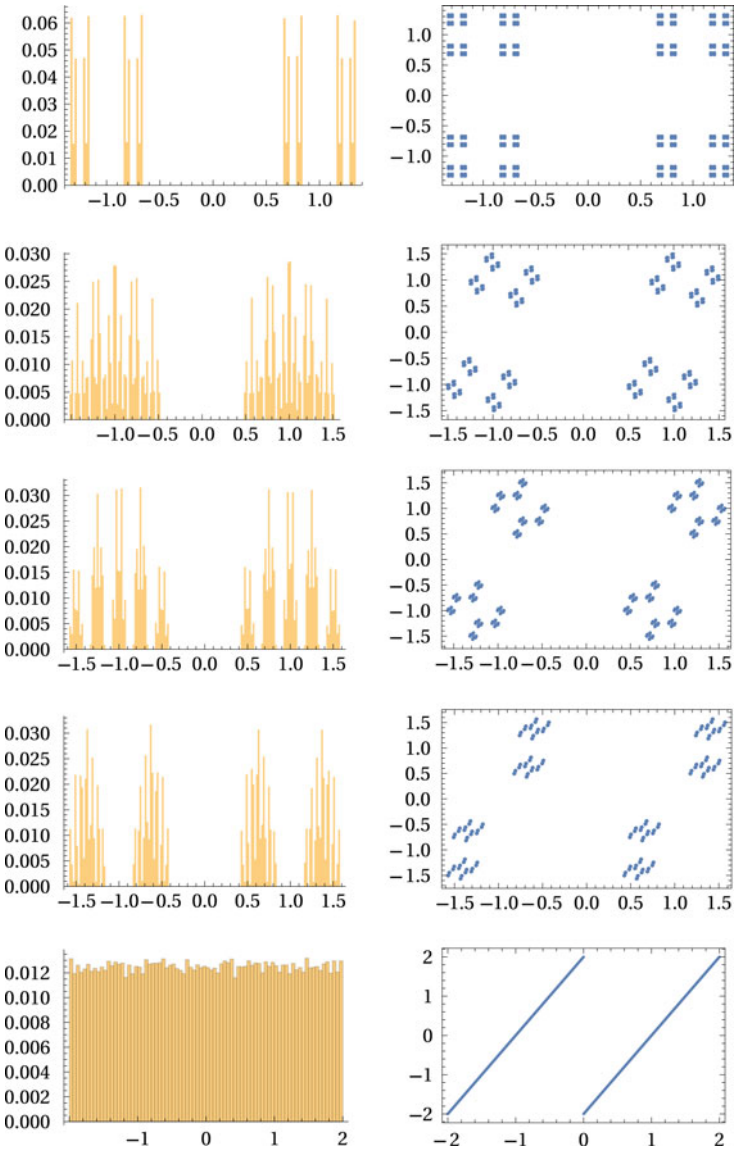


FIGURE 6. Histograms and recurrence plots fixed at $x = 0, \frac{1}{4}, \frac{1}{2}, \frac{3}{4}, 1$.

Similar to the construction of the case $T_n(0)$, we start from the interval $[-\sum_{i=0}^{\infty}\frac{|T_i(x)|}{2^i}, \sum_{i=0}^{\infty}\frac{|T_i(x)|}{2^i}]$, first removing the $(-1+\sum_{i=1}^{\infty}\frac{|T_i(x)|}{2^i}, 1-\sum_{i=1}^{\infty}\frac{|T_i(x)|}{2^i})$ interval. In the nth step let $a_1, a_2, \ldots, a_N$ denote the ascending sequence of different numbers $\sum_{i=0}^{n-1}\pm\frac{T_i(x)}{2^i}$. Let $L = \sum_{i=n}^{\infty}\frac{|T_i(x)|}{2^i}$ if $\frac{|T_n(x)|}{2^n} - \sum_{i=n+1}^{\infty}\frac{|T_i(x)|}{2^i} = l > 0$.

If the interval $(\max\{a_k - l, a_{k-1} + L\}, \min\{a_k + l, a_{k+1} - L\})$ is nonempty, its points can not be written as $\sum_{i=0}^{\infty}\frac{T_i(x)}{2^i}$. Hence we remove these intervals for $k = 1, \ldots, N$ (with $a_0 = -2 - L$ and $a_{N+1} = 2 + L$). Continuing this process for all n, we reach a complicated Cantor set. As $\frac{T_n(x)}{2^n}$ can be equal to $\sum_{i=n+1}^{\hat{n}}\pm\frac{T_i(x)}{2^i}$, the distribution will not be uniform.

The above examples show a wide spectrum of behaviour.

https://doi.org/10.1017/S0956792518000670 Published online by Cambridge University Press

4 Conclusions

Contrary to the prevalent notion that nonlinearity is a necessary ingredient for complex behaviour, chaotic motions also occur in infinite dimensional linear systems. Starting from Rolewicz's example of twice the backward shift on l_2, we constructed the corresponding shift operator $\mathcal{C}$ on $L_2\left(-1, 1, \left(1-x^2\right)^{-1/2}\right)$ and provided its representation using Cauchy's PV integral. We explicitly calculated the periodic points of the operator (including its nontrivial fixed point) and provided examples of bounded, unbounded and chaotic trajectories of $\mathcal{C}$. Histograms and recurrence plots of shifts of random Chebyshev expansions display interesting behaviour over fractal measures.

Acknowledgement

The research reported in this paper was supported by the Higher Education Excellence Program of the Ministry of Human Capacities in the frame of Water science & Disaster Prevention research area of Budapest University of Technology and Economics (BME FIKP-VÍZ).

References

[1] Bayart, F. & Matheron, É. (2009) *Dynamics of Linear Operators*, Vol. 179, Cambridge University Press, Cambridge, UK.
[2] Bernardes, N. C., Bonilla, A., Müller, V. & Peris, A. (2015) Li–Yorke chaos in linear dynamics. *Ergod. Theory Dyn. Syst.* **35**(6), 1723–1745.
[3] Bourdon, P. & Shapiro, J. H. (1997) *Cyclic Phenomena for Composition Operators*, Vol. 596, American Mathematical Society.
[4] Boyd, J. P. (2001) *Chebyshev and Fourier Spectral Methods*, Courier Corporation. Dover Publications, Mineola, NY.
[5] Bronshtein, I. N. & Semendyayev, K. A. (2013) *Handbook of Mathematics*, Springer Science & Business Media.
[6] Chan, K. C. (2002) The density of hypercyclic operators on a Hilbert space. *J. Operat. Theor.* **47**(1), 131–142.
[7] Conejero, J. A., Lizama, C. & Escribá, F. D. A. R. (2015) Chaotic behaviour of the solutions of the Moore-Gibson-Thompson equation. *Appl. Math. Inf. Sci.* **9**(5), 2233–2238.
[8] Desch, W., Schappacher, W. & Webb, G. F. (1997) Hypercyclic and chaotic semigroups of linear operators. *Ergod. Theory Dyn. Syst.* **17**(4), 793–819.
[9] Dyson, J., Villella-Bressan, R. & Webb, G. (1997) Hypercyclicity of solutions of a transport equation with delays. *Nonlinear Anal. Theory Methods Appl.* **29**(12), 1343–1351.
[10] Elliott, D. (1963) A Chebyshev series method for the numerical solution of Fredholm integral equations. *Comput. J.* **6**(1), 102–112, doi:10.1093/comjnl/6.1.102.
[11] Emamirad, H. (1998) Hypercyclicity in the scattering theory for linear transport equation. *Trans. Am. Math. Soc.* **350**(9), 3707–3716.
[12] Feldman, N. S. (2001) Linear chaos. *preprint*.
[13] Fu, X.-C. & Duan, J. (1999) Infinite-dimensional linear dynamical systems with chaoticity. *J. Nonlinear Sci.* **9**(2), 197–211.
[14] Gakhov, F. D., Sneddon, I. N., Stark, M. & Ulam, S. (2014) *Boundary Value Problems*, International Series in Pure and Applied Mathematics, Elsevier Science.
[15] Gethner, R. M. & Shapiro, J. H. (1987) Universal vectors for operators on spaces of holomorphic functions. *Proc. Am. Math. Soc.* **100**(2), 281–288.
[16] Gil, A., Segura, J. & Temme, N. M. (2007) *Numerical Methods for Special Functions*, SIAM e-books, Society for Industrial and Applied Mathematics (SIAM), Philadelphia, PA.

https://doi.org/10.1017/S0956792518000670 Published online by Cambridge University Press

[17] GODEFROY, G. & SHAPIRO, J. H. (1991) Operators with dense, invariant, cyclic vector manifolds. *J. Funct. Anal.* **98**(2), 229–269.
[18] GROSSE-ERDMANN, K.-G. & MANGUILLOT, A. P. (2011) *Linear Chaos*, Springer Science & Business Media.
[19] GULISASHVILI, A. & MACCLUER, C. R. (1996) Linear chaos in the unforced quantum harmonic oscillator. *J. Dyn. Syst. Meas. Control* **118**(2), 337–338.
[20] HAHN, S. L. (1996) *Hilbert Transforms in Signal Processing*, Artech House Signal Processing Library, Artech House, Boston, MA.
[21] HERRERO, D. A. (1992) Hypercyclic operators and chaos. *J. Operat. Theor.* **28**(1), 93–103.
[22] HOU, B., TIAN, G. & ZHU, S. (2012) Approximation of chaotic operators. *J. Operat. Theor.* **67**(2), 469–493.
[23] KALMÁR-NAGY, T. & KISS, M. (2017) Complexity in linear systems: a chaotic linear operator on the space of odd 2π-periodic functions. *Complexity* **2017**, doi:10.1155/2017/6020213.
[24] KING, F. W. (2009) *Hilbert Transforms*, 1st ed., Vol. 1, Encyclopedia of Mathematics and its Applications. Cambridge University Press, Cambridge, doi:10.1017/CBO9780511721458.
[25] KOWALSKI, K. & STEEB, W.-H. (1991) *Nonlinear Dynamical Systems and Carleman Linearization*, World Scientific.
[26] KRANTZ, S. G. (2009) *Explorations in Harmonic Analysis: With Applications to Complex Function Theory and the Heisenberg Group*, 1st ed., Applied and Numerical Harmonic Analysis, Birkhäuser Basel.
[27] MACCLUER, C. R. (1992) Chaos in linear distributed systems. *J. Dyn. Syst. Meas. Control* **114**(2), 322–324.
[28] MARTÍNEZ-GIMÉNEZ, F., OPROCHA, P. & PERIS, A. (2013) Distributional chaos for operators with full scrambled sets. *Mathematische Zeitschrift* **274**(1–2), 603–612.
[29] MARTÍNEZ-GIMÉNEZ, F. & PERIS, A. (2002) Chaos for backward shift operators. *Int. J. Bifurcat. Chaos* **12**(8), 1703–1715.
[30] PROTOPOPESCU, V. & AZMY, Y. Y. (1992) Topological chaos for a class of linear models. *Math. Models Methods Appl. Sci.* **2**(1), 79–90.
[31] ROLEWICZ, S. (1969) On orbits of elements. *Stud. Math.* **32**(1), 17–22.
[32] SADOSKY, C. (1979) *Interpolation of Operators and Singular Integrals: An Introduction to Harmonic Analysis*, Monographs and Textbooks in Pure and Applied Mathematics, Marcel Dekker Inc.
[33] SALAS, H. N. (1995) Hypercyclic weighted shifts. *Transactions of the American Mathematical Society* **347**(3), 93–1004.
[34] SHAPIRO, J. H. (2001) *Notes on the Dynamics of Linear Operators*. Unpublished Lecture Notes (available at www.math.msu.edu/shapiro).

https://doi.org/10.1017/S0956792518000670 Published online by Cambridge University Press